CORE TRANSPORT MODELING AND CHARACTERIZATION FOR COMPACT TOKAMAK REACTOR SCENARIOS

C. HOLLAND, E.M. BASS, D. ORLOV
Center for Energy Research, University of California, San Diego
La Jolla, CA, United States
Email: chholland@ucsd.edu

J. MCCLENAGHAN, B.C. LYONS, X. JIAN, B.A. GRIERSON
General Atomics
San Diego, CA, United States

N.T. HOWARD, P. RODRIGUEZ-FERNANDEZ
MIT Plasma Science and Fusion Center
Cambridge, MA, Unites States

Abstract

Motivated by the current interest in compact, high-field approaches to fusion power plants, the OMFIT STEP integrated modeling workflow has been used to generate self-consistent core plasma transport solutions representative of potential compact tokamak reactor operating scenarios. In this study, solutions for an idealized R_{maj} = 4 m, B_0 = 8 T tokamak "use case reactor" (UCR) were developed, with the intention of providing starting parameters for more comprehensive future transport studies in the spirit of the CYCLONE base case. Both inductive pulsed (UCR-P) and steady-state (UCR-SS) solutions potentially capable of producing 1 GW of fusion power and 200 MW or more net electric power have been identified. A common feature of both scenarios is that the core confinement time is long enough for the plasmas to be well-coupled, even though core collisionality is low. This situation leads to significant core ion thermal transport, despite the heating being predominantly to the electrons, and a corresponding dominance of long-wavelength ion temperature gradient modes. A similar situation is found to hold for ITER and SPARC plasma scenarios, and is argued to be an inherent property of power plant-relevant burning plasmas. For both UCR scenarios, the EPED code predicts peeling-limited pedestals with extremely weak sensitivity to core pressure values, enabling use of a fixed boundary condition in core transport modeling. With this constraint, another key finding of this study is the extreme sensitivity of the results to the quantitative stiffness level of the transport model used as well as the predicted critical gradients, with outcomes ranging from runaway ignition to radiative collapse possible depending upon the choice of TGLF saturation rule. Given this uncertainty, new analysis presented in the paper details initial benchmarking of TGLF against linear and nonlinear gyrokinetic simulations. The gyrokinetic results are broadly consistent with the relevant TGLF predictions, but highlight the need to improve the accuracy of transport stiffness and particle flux predictions, especially at larger radii.

1. INTRODUCTION

Around the world, there is increasing public and private interest in accelerating the development of fusion energy as a source of greenhouse gas emission-free energy source. Towards this end, a variety of different concepts for a fusion pilot plant (FPP) are being investigated, with the aim of demonstrating an accelerated path to net electricity production at commercially relevant scales and costs. Many of these concepts focus on providing "compact" devices that aim to produce several hundred MW of net electric power at substantially reduced capital cost than envisioned for previous GW-class reactors [1-6], leveraging advances in technology and scientific understanding. Developing commercial fusion power on the desired timeline (e.g. of the recent Bold Decadal Vision [7]) will require extensive use of validated predictive modelling capabilities to move almost directly from current devices to first-of-a-kind FPPs, as there is very limited time to construct and operate multiple intermediate research, development, and testing facilities.

To help inform the design of such FPPs, the OMFIT STEP integrated modelling workflow [8-10] has been used to generate self-consistent core plasma transport solutions representative of potential compact tokamak reactor operating scenarios. Rather than obtaining specific design conclusions, the guiding intention of this study was to develop an initial characterization of dominant transport processes at reactor-relevant conditions, and formulate starting parameters for more comprehensive future transport studies in the spirit of the CYCLONE

base case. In this study, solutions for an idealized R_{maj} = 4 m, B_0 = 8 T tokamak "use case reactor" (UCR) were developed. Both inductive pulsed (UCR-P) and steady-state (UCR-SS) solutions potentially capable of producing 1 GW of fusion power and 200 MW or more net electric power were identified (Fig. 1). The full details of these scenarios, including how parameters were determined, and a comprehensive investigation of the impacts of different physics and model choices, were recently published in Ref. 11.

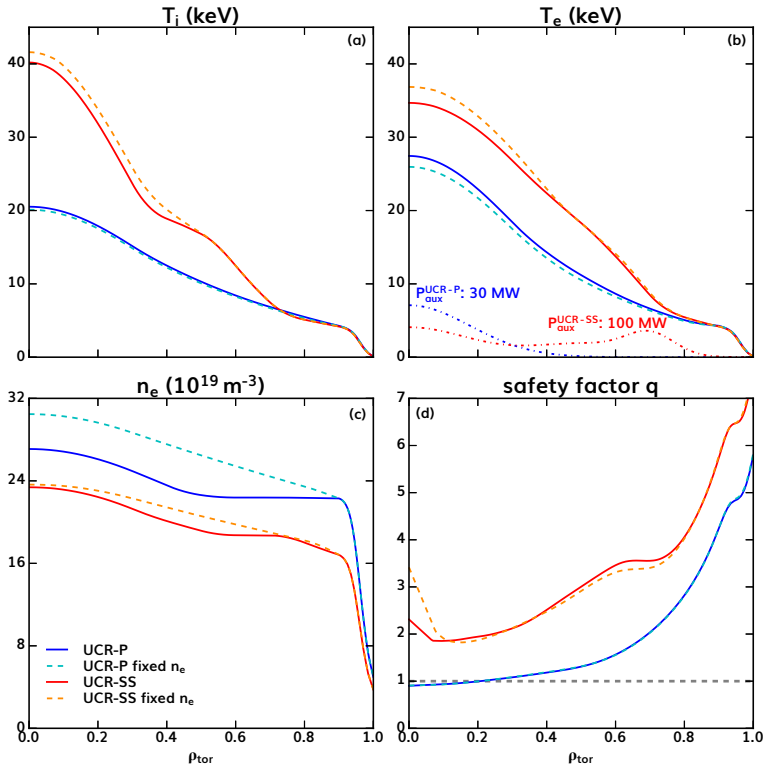

Fig. 1. Comparison of predicted UCR-P and UCR-SS profiles of (a) ion temperature T_i, (b) electron temperature T_e, (c) electron density n_e, and (d) safety factor q. Reproduced with permission from Ref. 11.

The remainder of the paper is structured as follows. In Section 2, the key characteristics of the UCR transport solutions are reviewed, and compared to other burning plasma predictions. Based on these results, a heuristic model of transport in commercially-relevant magnetically confined burning plasmas is proposed. In Section 3, a more quantitative analysis of transport in the inductive UCR-P scenario is presented, illustrating the impact of transport stiffness on the predictions and comparing gyrokinetic and gyrofluid predictions for this scenario. Conclusions and future work directions are discussed in Section 4.

2. CONTROLING ROLE OF ION TEMPERATURE GRADIENT MODES IN MAGNETICALLY CONFINED BURNING PLASMAS

The recently published UCR study [11] focused on identifying relatively self-consistent H-mode core transport solutions plasmas with R_{maj} = 4 m, minor radius a = 1.4 m, elongation κ = 2, triangularity δ = 0.5, $Z_{eff} \sim 2$ and on-axis magnetic field B_0 = 8 T. Additional constraints were that the pedestal density be no more than 80% of the Greenwald density $n_G = I_p/\pi a^2$ and edge safety factor $q_{95} > 5$, to reduce likelihood of disruptions, and only radiofrequency-like external actuators which provide electron heating and current drive (but not fueling or ion heating) be used. Additionally, plasmas which could produce at least 200 MW net electric power were sought. Details of the assumptions on various efficiencies made to relate the net electric power P_{net} to P_{fus} can be found in Appendix A of Ref. 10, with the upshot being an effective relationship of

$$P_{net} \approx (0.35*Q_{fusion} - 2.3)* P_{aux} \quad (1)$$

where P_{aux} is the amount of heating power absorbed by the plasma. The near-edge pedestal properties were determined via EPED [12,13], and core profile predictions made using the TGYRO code [14], with TGLF [15] and NEO (for the steady-state case) [16,17] used to calculate turbulent and neoclassical transport. Unless otherwise stated, the TGLF SAT1 rule [18] with perpendicular magnetic fluctuations included was used for this analysis. The magnetic equilibrium was calculated using the CHEASE code [19], and current diffusion and classical α-particle distributions with ONETWO [20].

Within these constraints, both an inductive scenario at I_p = 16 MA, P_{aux} = 30 MW and steady-state scenario at I_p = 12 MA, P_{aux} = 100 MW were identified (Fig. 1). In both cases, EPED predicted the pedestals to be peeling-limited, with essentially no dependence on $\beta_n = \beta/(I_p/aB)$ (where $\beta = 2\mu_o p/ B_0^2$). Although the plasmas satisfied all the targets identified above, their viability from a resistive MHD stability and core-edge integration standpoint requires further analysis and possible refinement. Notably, no toroidal rotation is assumed to arise or be driven, so the robustness of the plasmas to e.g. resistive wall mode and/or neoclassical tearing mode locking remains uncertain. Furthermore, while the steady-state scenario is predicted to have an exhaust power well above the L-H threshold, the pulsed scenario does not. The sensitivity of these results to variations in impurity mix, and more accurate modelling/optimization of the pedestal profiles, also remains to be undertaken.

One of the most interesting features of these scenarios is that although the heating (both external and via fusion) is dominantly to the electrons, ion thermal transport is as large as, or larger than, electron thermal transport in both scenarios. Examination of equivalent transport modelling results for a number of other burning plasmas including the inductive ITER baseline scenario [21] and SPARC primary reference discharge [22] finds a similar situation holds. To understand this result, a heuristic model is shown in Fig. 2, which is proposed to be applicable to any magnetically confined burning D-T plasma. The key elements of this model are as follows:

a) By definition in a burning plasma, alpha heating must dominate over auxillary sources, and at virtually all temperatures of interest, this heating will predominantly go to the electrons.
b) The dominant electron heating raises T_e above T_i, thus leading to collisional exchange heating of the ions from the electrons.
c) In order to keep the ions hot enough to sustain the fusion burn, a significant amount of the α-heating must be coupled back into the ions, and so the plasma must be sufficiently well-coupled that the energy confinement time is long relative to the exchange time.
d) Once heat is "in" the core ions, it must move outward via transport, as radiative losses only cool the electrons. For burning plasma conditions, the ion collisionality is sufficiently low that this transport is almost always turbulent, rather than neoclassical, in nature.
e) Near the separatrix, there is a point where the plasma switches from $T_e > T_i$ to $T_i > T_e$ as radiation and parallel conduction in the scrape-off layer rapidly cool off the electrons. In this region, exchange process is reversed, with energy flowing back into the electrons from the ions.

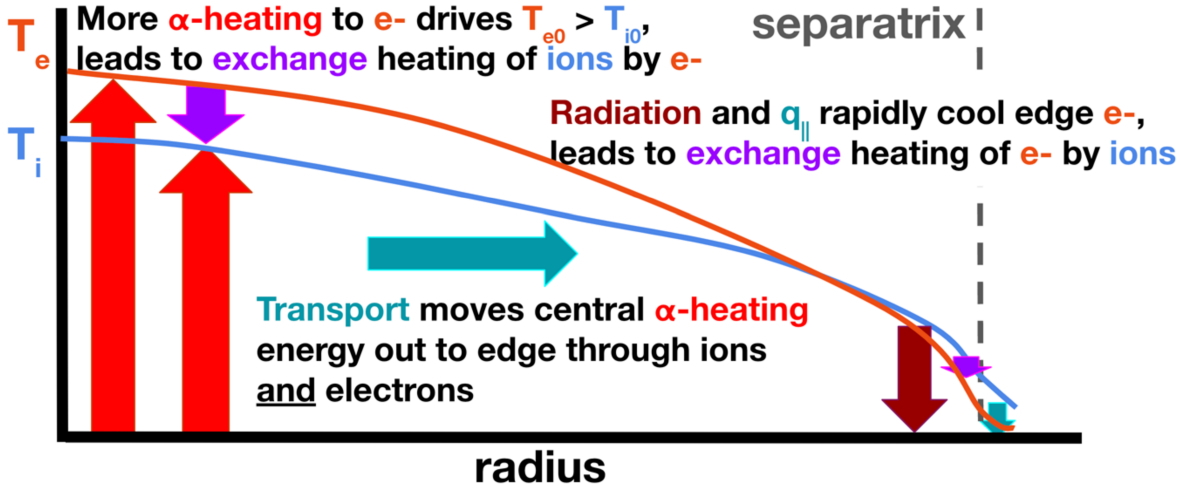

Fig. 2. Illustration of the heuristic model of self-consistent power flows in a D-T reactor. Reproduced with permission from Ref. 11.

While certainly there are quantitative limits to the assumptions made here, the picture presented above appears to at least qualitatively well-describe a number of burning plasma scenarios in devices of different size and field. Moreover, this model suggests some quantitative metrics that can be used to more rigorously test its assumptions. The first is to examine the ratio of energy confinement time to core volume-averaged exchange time, as a measure of how well-coupled the plasma is. The second is to look at the core volume-averaged ratio of ion to electron turbulent fluxes or thermal diffusivities, as a way of "fingerprinting" (in the language of Kotschenreuther *et al*. [23]) the dominant core transport mechanism. An initial calculation of these metrics is shown in Fig. 3 for a number of burning plasmas and current-day DIII-D experiments. As shown in Fig. 3a, all but one of these plasmas have at least 50% or more of their total heating to the electrons. However, when considering the ratio of fluxes (Fig. 3b) or especially turbulent thermal diffusivities (Fig. 3c), the situation reverses to one where turbulent ion thermal transport clearly plays a significant, if not dominant, role in setting the overall transport of the system.

Following the fingerprint paradigm of Kotschenreuther *et al*. further, there are effectively only two burning-plasma relevant turbulent transport modes consistent with this scenario- the ion temperature gradient (ITG) mode, and the kinetic ballooning mode (KBM). While both can potentially provide the relevant thermal fluxes, it is generally assumed that only the ITG mode is likely to have a capability for driving a particle pinch. Given the strong desirability, if not need, for peaked density profiles to provide increase fusion power and bootstrap currents, it appears that ITG-dominated plasmas are the most likely to be consistent with requirements for operating a sustained burning plasma. While this assertion does not rule out potential roles for KBMs or shorter-wavelength trapped electron modes (TEMs) or electron temperature gradient (ETG) modes in burning plasmas, it does argue that such modes cannot dominant the transport in volume-average sense.

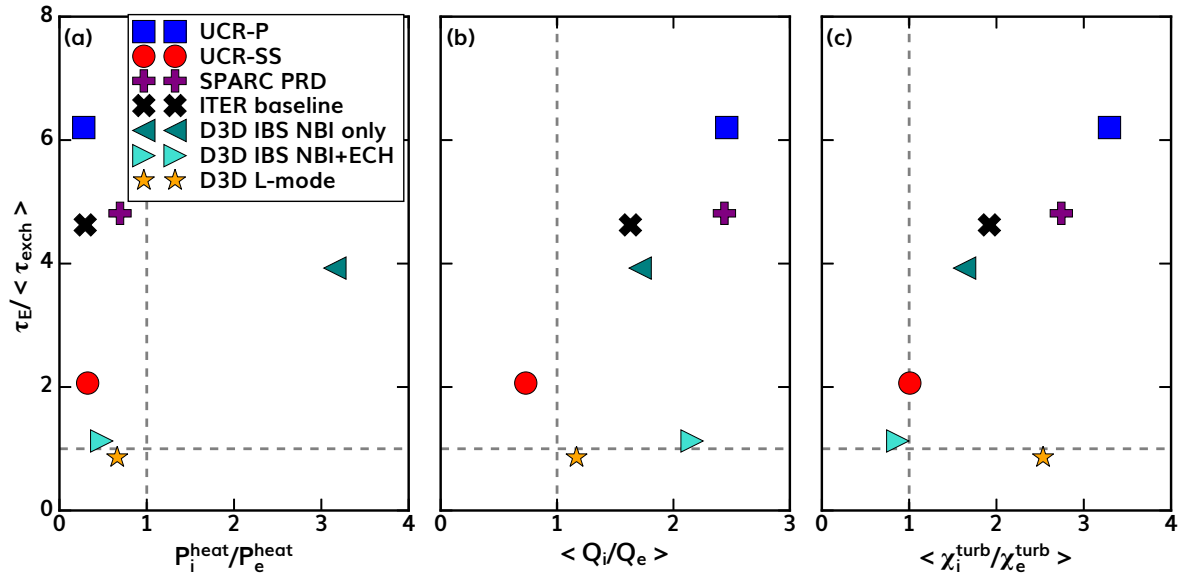

Fig. 3. Comparison of the coupling metric $\tau_E/\langle\tau_{exch}\rangle$ as a function of the ratio of ion to electron (a) heating, (b) power fluxes, and (c) turbulent diffusivities for a variety of different current and future plasmas. Brackets denote a volume-weighted averaged over the core region of $0 \leq \rho_{tor} \leq 0.9$. Reproduced with permission from Ref. 11.

3. BENCHMARKING GYROFLUID AND GYROKINETIC PREDICTIONS IN THE UCR-P SCENARIO

One key feature of the ITG instability, and the resulting turbulence, is the existence of a critical value of the normalized driving gradient $R/L_{Ti} = -(R/T_i)dT_i/dr$ that must be exceed for finite growth rate and transport. A second key feature is strong ITG stiffness- a rapid increase in growth rate and/or turbulent fluxes as R/L_{Ti} increases above the critical value. The implied consequence is that one would expect "infinitely" stiff ITG turbulence to pin the experimental R/L_{Ti} profile (and thus T_i) to the critical value, regardless of the actual power to be conducting. In practice, ITG transport is often found to be stiff but not infinitely so, such that predicted

temperature profiles and reactor performance can depend sensitively on both the critical gradient and level of stiffness above that gradient. Such is the situation for the UCR plasmas. For the pulsed UCR-P case, the choice of TGLF saturation rule (each of which predicts a different stiffness, but nearly the same critical gradient, as shown in Ref. 10) can lead to dramatically different results, as seen in Fig. 4. Indeed, for the least stiff model (SAT0), UCR-P essentially ignites, whereas for the most stiff model (SAT2 [24]), the plasma suffers a radiative collapse (and does not collapse further only due to the assumption of a fixed pedestal). Even more pronounced impacts are found for the UCR-SS case, with completely different heating mixes, plasma currents, and pedestal conditions apparently needed for each saturation rule to obtain self-consistent solutions.

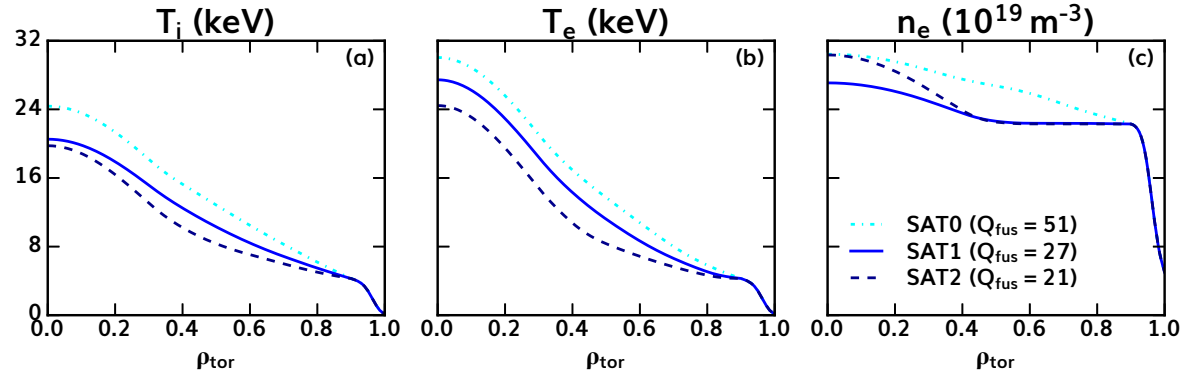

Fig. 4. Comparison of predicted temperature and density profiles for the UCR-P scenario as a function of TGLF saturation rule, illustrating the impact of increased transport stiffness from SAT0 to SAT2 on fusion gain. Reproduced with permission from Ref. 11.

Given the impact of saturation rule choice on the predicted results, it is imperative to benchmark the TGLF predictions against higher fidelity models, in this case gyrokinetics. Fig. 5 shows a comparison of linear growth rate and frequency between different gyrofluid predictions made by TGLF saturation rules and gyrokinetic predictions made with the CGYRO code [25], for the UCR-P plasma at ρ_{tor} = 0.3 and 0.7, where ρ_{tor} is the square root of toroidal flux normalized to its separatrix value. The corresponding scalings of the linear growth rate and frequency for normalized binormal wavenumber $k_y\rho_s$ = 0.3 with increasing temperature gradient is shown in Fig. 4**.** Here $k_y = nq/r_{min}$ with n the torodial modenubmer, and $\rho_s = c_s/\Omega_{ci}$, with Ω_{ci} calculated using B_{unit} as defined in Ref. 25.

Examination of both figures indicates that at ρ_{tor} = 0.7 TGLF provides a reasonable estimate of the ITG growth rate and frequency, as well as the critical gradient and scaling with R/L_{Ti} above it. However, at that radius both saturation rules predict unstable TEM modes at higher k_y not seen in the gyrokinetic calculations. This overprediction of TEM modes around $k_y\rho_s \sim 1$ has been seen in previous studies as well. In contrast, at ρ_{tor} = 0.3 both saturation rules predict substantially larger linear mode characteristic differences from the gyrokinetic results than at ρ_{tor} = 0.7. In this case, TGLF also does not observe the strongly unstable modes at the longest wavelengths ($k_y\rho_s$ = 0.1 and 0.2) which propagate in the electron diamagnetic direction predicted by CGYRO, and again predicts a transition to robustly unstable electron modes above $k_y\rho_s$ = 0.5 not seen by CGYRO. The exact nature of the long wavelengths modes is under investigation. As they maintain a ballooning-like eigenmode structure they are unlikely to be microtearing modes, while propagation in the electron direction is inconsistent with expectations for conventional KBMs. More broadly, there are a number of potential sources for the larger TGLF-CGYRO discrepancy at ρ_{tor} = 0.3, including the relatively low magnetic shear (s = 0.26), large local β ($\beta_{e,unit}$ = 0.014), and low collisionality (υ_{ei} = 0.01 c_s/a). Which of these or other potential mechanisms drives the differences remains to be determined.

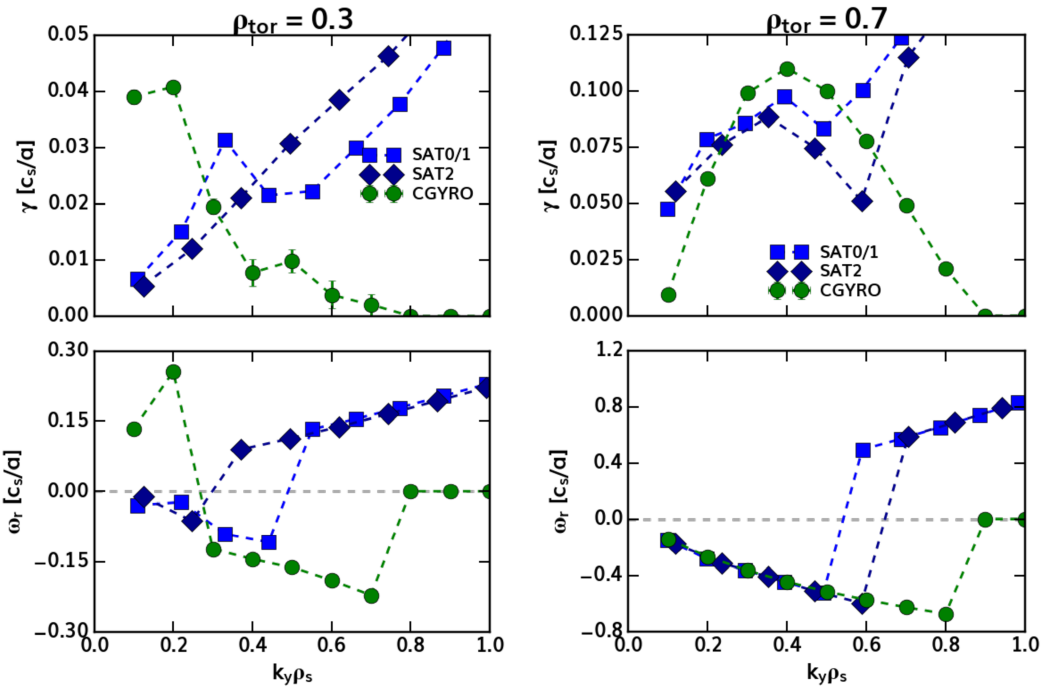

Fig. 5. CGYRO and TGLF predictions of linear growth rate γ_{lin} (top) and real frequency ω_r (bottom) vs. $k_y\rho_s$ at ρ_{tor} = 0.3 (left) and 0.7 (right).

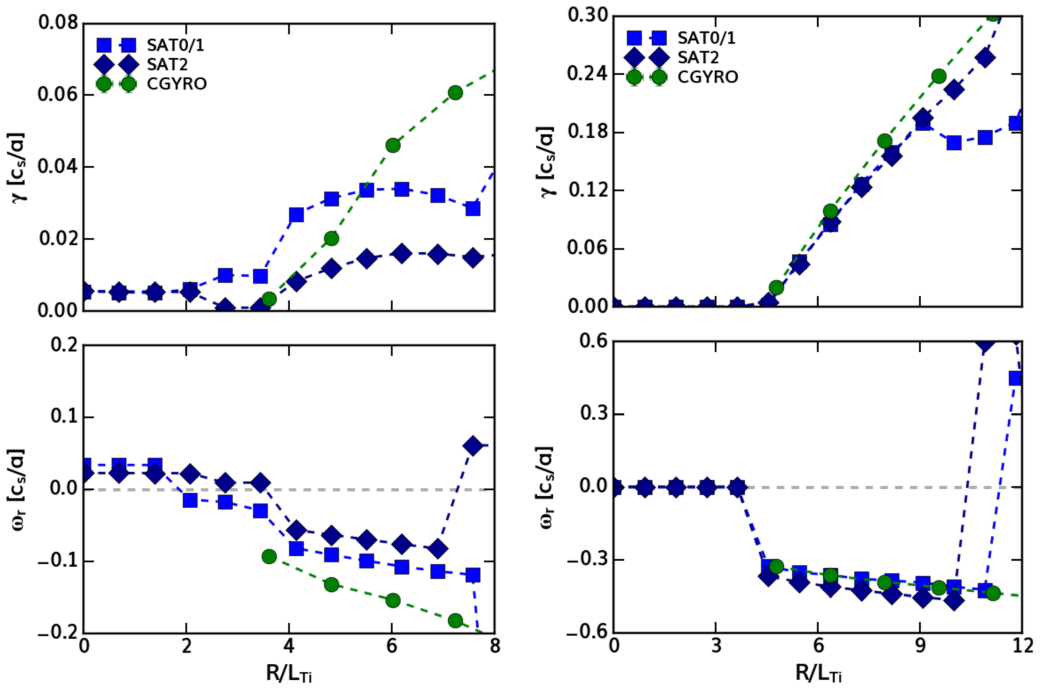

Fig. 6. CGYRO and TGLF predictions of linear growth rate γ_{lin} (top) and real frequency ω_r (bottom) vs. R/L_{Ti} for $k_y\rho_s$ = 0.3 at ρ_{tor} = 0.3 (left) and 0.7 (right). R/L_{Te} was proportionally rescaled from the nominal value by the same amount as R/L_{Ti}.

Building on the linear results, a set of initial nonlinear runs has been performed at these radii, to compare gyrofluid and gyrokinetic predictions of transport stiffness. The results are shown in Fig. 7, and largely correspond to what would be expected from the linear analysis. At ρ_{tor} = 0.3, the plasma exhibits extremely stiff behaviour above a critical gradient relatively close to the linear threshold. The nonlinear results at this radius also appear to be dominated by ITG modes, with no obvious evidence for the linearly unstable long-wavelength

modes with phase velocities in the electron diamagnetic direction. Most importantly from a integrated modelling perspective, the power-balance fluxes in gyroBohm normalized units (where $Q_{gB} = n_e T_e c_s (\rho_s/a)^2$) are sufficiently small that the predicted level of transport stiffness is less important than the predicted critical gradient for onset.

While accurate prediction of the critical gradient remains essential at $\rho_{tor} = 0.7$, the larger normalized power balance fluxes at this radius mean that the quantitative stiffness of the predicted transport also plays an important role in setting the predicted profile gradients here. As can be seen from the right column of Fig. 7, both TGLF saturation rules and nonlinear CGYRO simulations predict similar critical R/L_{Ti} values for the onset of turbulent transport. However, the differences is stiffness between the three curves predicts significant differences in what R/L_{Ti} would be in the scenario in order to provide the necessary transport. Moreover, although CGYRO predicts thermal transport stiffness between the SAT1 and SAT2 predictions, it also predicts a stronger particle pinch than either SAT1 or SAT2. Thus, a self-consistent solution made using CGYRO is likely to organize to a higher density gradient state, which will in turn lead to changes in the power balance fluxes (both in absolute and normalized units) as well as ITG stability. Improving the accuracy of these predictions at is particularly important for integrated modelling because even small changes in scale lengths at larger radii are magnified as their impact propagates into the core parameters. For instance, even a slight increase in density gradient at $\rho_{tor} = 0.7$ corresponds to higher density at all $\rho_{tor} < 0.7$. Self-consistent gyrokinetic profile predictions for the UCR-P and ARC V1C [26] inductive scenarios are currently underway using the PORTALS framework [27], and will be reported in the near future.

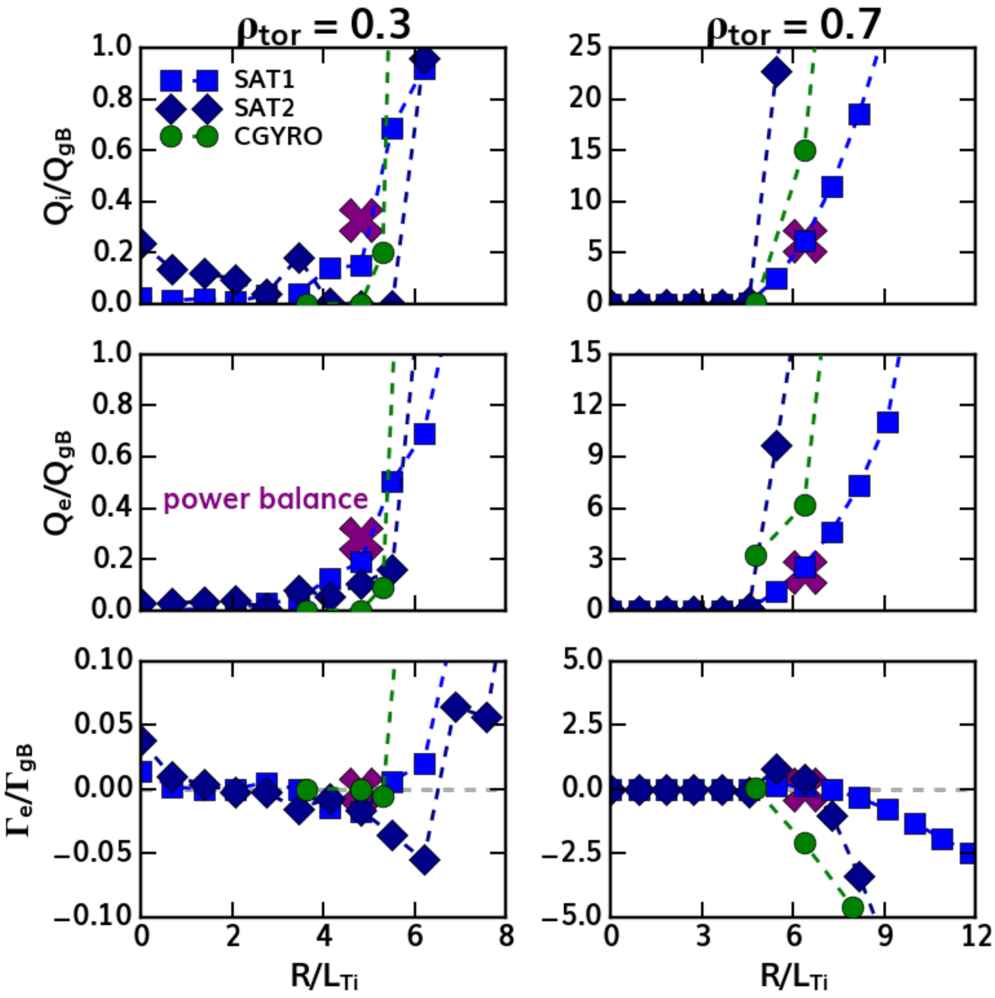

Fig. 7. CGYRO and TGLF Q_i (top), Q_e (middle), Γ_e (bottom) vs. R/L_{Ti} at $\rho_{tor} = 0.3$ (left) and 0.7 (right). R/L_{Te} was proportionally rescaled from the nominal value by the same amount as R/L_{Ti}.

4. CONCLUSIONS

Developing viable operating scenarios for an FPP requires balancing many competing physics, engineering, and economic constraints. In the case of a D-T tokamak FPP, the analysis presented here suggests that core plasma confinement is very likely to be dominated by ITG turbulence. This conclusion has the upside that the ITG mode is perhaps the most well-studied and understood instability in tokamaks. The less positive implication is that control and optimization of ITG in current day systems typically relies upon external actuators such as significant torque injection via neutral beams, or weakly coupled scenarios with $T_i/T_e > 1$, that do not scale well to burning plasmas. Nonetheless, the UCR scenario study suggests that even with these constraints, there are plausible ITG-dominant targets for compact high field FPPs, that can likely be further optimized. A key aspect in doing so will be to revisit the analysis of both the inductive and steady-state design using direct gyrokinetic calculations, to make more accurate predictions of thresholds, transport stiffness, and particle fluxes.

ACKNOWLEDGEMENTS

This work was funded by the U.S. Department of Energy Award Nos. DE-SC001828, DE-FG02-95ER54309, DE-SC0017992, DE-SC0014264, and DE-SC0023108. This research used resources of the National Energy Research Scientific Computing Center (NERSC), a U.S. Department of Energy Office of Science User Facility located at Lawrence Berkeley National Laboratory, operated under Contract No. DE-AC02-05CH11231, and the Engaging cluster at the MGHPCC facility that was funded by Award No. DE-FG02-91-ER54109.

REFERENCES

[1] NAJMABADI, F. et al, *Fus. Eng. Design* **80** (2006) 3
[2] WAN, B. et al, *IEEE Transactions on Plasma Science* **42** (2014) 495
[3] KESSEL, C. E. et al, *Fusion Science and Technology* **67** (2015) 1
[4] KANG, J. S. et al, *Nucl. Fusion* **57** (2017) 126034
[5] TOBITA, K. et al, *Fusion Science and Technology* **75** (2019) 372
[6] FEDERICI, G., HOLDEN, J., BAYLARD, C. and BEAUMONT, A., *Fus. Eng. Design* **173** (2021) 112959
[7] https://www.whitehouse.gov/ostp/news-updates/2022/04/19/readout-of-the-white-house-summit-on-developing-a-bold-decadal-vision-for-commercial-fusion-energy/
[8] MENEGHINI, O. et al, *Nucl. Fusion* **55** (2015) 083008
[9] MENEGHINI, O. et al, *Nucl. Fusion* **10** (2020) 1088
[10] LYONS, B. C. et al, *Phys. Plasmas* **25** (2018) 056111
[11] HOLLAND, C. et al, *J. Plasma Phys.* **89** (2023) 905890418
[12] SNYDER, P. B. et al, *Phys. Plasmas* **16** (2009) 056118
[13] SNYDER, P. B. et al, *Nucl. Fusion* **51** (2011) 103016
[14] CANDY, J. et al, *Phys. Plasmas* **16** (2009) 060704
[15] STAEBLER, G. M., KINSEY, J. E. and WALTZ, R. E., *Phys. Plasmas* **14** (2007) 055909
[16] BELLI, E. A. and CANDY, J., *Plasma Phys. Cont. Fusion* **50** (2008) 095010
[17] BELLI, E. A. and CANDY, J., *Plasma Phys. Cont. Fusion* **54** (2012) 015015
[18] STAEBLER, G. M., CANDY, J., HOWARD, N. T., and HOLLAND, C., *Phys. Plasmas* **23** (2016) 062518
[19] LÜTJENS, H., BONDESON, A., and SAUTER, O., *Computer Physics Communications* **97** (1996) 219
[20] ST. JOHN, H., TAYLOR, T. S., LIN-LIU, Y. R., and TURNBULL, A. D., *Plasma Physics and Controlled Nuclear Fusion Research* **3** (1994) 603
[21] MANTICA, P. et al., *Plasma Phys. Cont. Fusion* **62** (2020) 014021
[22] RODRIGUEZ-FERNANDEZ, P. et al, *Nucl. Fusion* **62** 0(2022) 42003
[23] KOTSCHENREUTHER, M. et al., *Nucl. Fusion* **59** (2019) 096001
[24] STAEBLER, G. M. et al, *Nucl. Fusion* **61** (2021) 116007
[25] CANDY, J., BELLI, E. A., AND BRAVENEC, R. V., *J. Comp. Phys.* **324** (2016) 73
[26] CREELY, A. J., "SPARC as a Path to ARC and Commercial Fusion Power", JO07.00002, presented at 63rd Annual Meeting of the APS Division of Plasma Physics, Pittsburgh, PA (2021)
[27] RODRIGUEZ-FERNANDEZ, P. et al, *Nucl. Fusion* **62** (2022) 076036